JOURNAL OF MATERIALS SCIENCE 12 (1977) 2195–2199

A model for crack initiation in elastic/plastic indentation fields

B. R. LAWN
Department of Applied Physics, University of New South Wales, Kensington, New South Wales 2033, Australia

A. G. EVANS
Science Center, Rockwell International, Thousand Oaks, California 91360, USA

A model is proposed for the initiation of microfracture beneath sharp indenters. Using a simple approximation for the tensile stress distribution in the elastic/plastic indentation field, in conjunction with the principle of geometrical similarity, fracture mechanics procedures are applied to determine critical conditions for the growth of penny-like "median cracks" from sub-surface flaws. The analysis provides a functional relationship between the size of the critical flaw and the indentation load necessary to make this flaw extend. Initiation is well defined (unstable) only if the critical flaw lies within a certain size range; outside this range, large flaws can extend stably but small flaws can not extend at all. No flaws can extend below a characteristic minimum load, values of the indentation variables at this load accordingly providing useful threshold parameters. These quantities involve the intrinsic deformation/fracture parameters, hardness and toughness, in a fundamental way, thereby establishing a basis for materials selection in fracture-sensitive applications.

1. Introduction

The susceptibility of brittle materials to indentation cracking involves two major questions [1]: *initiation*, how and where in the indentation field the cracks start; *propagation*, once started, what paths do the cracks take, and what determines the extent of their growth. Of these two aspects, that of propagation is relatively well understood [1–3], for it is in this stage of growth that the fracture mechanics notion of a "well-developed" crack is most applicable. In the initiation stage the dependence of crack nucleation and formation processes on a multiplicity of structural and specimen history factors tends to introduce complications, among them the issue of flaw statistics. Nevertheless, with increasing attention being directed by the ceramics industry to such properties as surface erosion and degradation, especially in high-impact situations, the need for an understanding of contact-induced crack initiation is of paramount importance in preventative design.

Where the indenter in any given contact system can be considered "blunt" [1], such that the contact prior to well-developed fracture is perfectly elastic, the mechanics of initiation are reasonably straightforward. This situation is realized when a hard sphere is used to produce Hertzian "cone cracks" in highly brittle surfaces [4]. On loading the indenter, pre-present flaws on the specimen surface experience an ever-increasing tensile stress outside the expanding contact circle, until one such flaw becomes critical and develops spontaneously into the cone configuration. However, because this critical event involves overcoming an energy barrier, the threshold condition is found to be independent of any flaw characteristics, provided the density of flaws is sufficiently high. If the distribution of flaws becomes sparse, so that the contact has to continue expanding in its search for a suitable starting centre, the threshold load tends to increase and show variability: flaw statistics then enter the problem.

© *1977 Chapman and Hall Ltd. Printed in Great Britain.*

Where, on the other hand, the contact system is "sharp", such that the contact prior to fracture is "plastic"*, the mechanics of initiation become more obscure [5]. Yet it is the sharp indenter which is usually by far the more dangerous, with threshold loads typically some orders of magnitude less than that required for cone crack formation. The pyramidal and conical indenters used in routine hardness testing most conveniently idealize this second category of indentation fracture, although even a hard sphere is capable of precursor plastic penetration in less brittle surfaces [2, 3]. In this case the intensity of the stress field remains independent of applied load (except for the increase due to work-hardening with spherical indenters, where the principle of geometrical similarity does not apply), so that the existence of a threshold would appear to be necessarily connected with a critical spatial factor. Empirical evidence points to the operation of sub-surface crack sources, in the vicinity of the elastic/plastic boundary where tensile stresses concentrate; these form into penny-shaped "median cracks", as in Fig. 1, on any favourable symmetry planes through the indentation. At least, this is so for reasonably well finished surfaces: a rough finish may lead to the premature development of shallow surface "radial cracks" extending outward from the impression, particularly with spherical indenters [2, 3]. Ultimately, at higher loads, the median cracks tend to merge with any radial cracks to form well-developed half-penny configurations centred on the contact point [6]. One further development occurs on unloading, where "lateral cracks", driven by a residual, elastic/plastic mismatch stress field, extend sideways and toward the specimen surface [5]. While all of these crack types contribute to the final damage pattern, it is the median crack which is of greatest concern in the context of preventative design, for it is the onset of this mode which limits the indentation load that may be sustained by any given brittle surface without degradation (no matter how well prepared the surface may be).

Accordingly, this paper seeks to establish a working model for predicting the onset of median cracking beneath sharp indenters. Given that the initiation process is controlled by the elastic/plastic indentation field, we might intuitively expect intrinsic deformation/fracture parameters, notably hardness and toughness, to play an important part in the formulation [7, 8]. In showing this indeed to be the case, the present model lays down a convenient basis for materials selection.

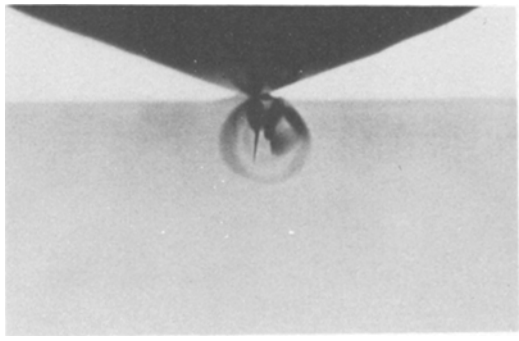

Figure 1 In situ photograph of Vickers diamond pyramid indentation in soda-lime glass, showing well-developed median crack at load 250 N. Side view in transmitted light, width of field 11 mm. (After [5].)

2. The model

The proposed model is illustrated in Fig. 2. A sharp indenter at load P produces a plastic impression of characteristic dimension a, from which one obtains the hardness,

$$H = P/\alpha\pi a^2 \approx \text{const.}, \qquad (1)$$

with α a dimensionless factor determined by indenter geometry. The elastic/plastic field in the general indentation problem is extremely complex, but Hill's solution for a spherical cavity under internal pressure illustrates the essential features of the stress distribution. The maximum tensile stress occurs at the elastic/plastic interface, with fall-off within the plastic zone to a negative value at the indenter/specimen contact and within the surrounding elastic region to zero remote from the contact [9]. The features pertinent to the fracture problem are most simply approximated by a linear profile, as shown in Fig. 2. Here σ_m is the maximum tension at the interface, depth d below the surface, and b is the spatial extent over which the tensile component of the field acts. In so far as the concept of geometrical similitude may be applied to the sharp-indenter field [10], H and a constitute convenient scaling parameters. The peak stress must scale directly with the indentation

*The term "plastic" being used loosely here to represent any irreversible deformation process, including densification.

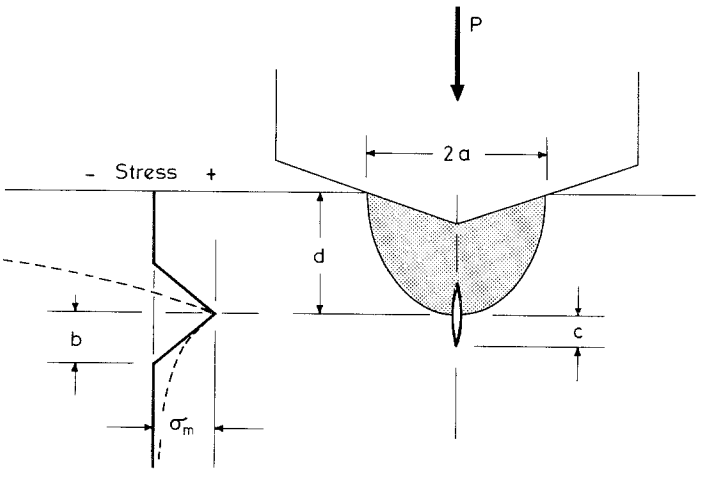

Figure 2 Model for median crack initiation in elastic/plastic indentation field. Nucleation centre is located in region of maximum tension, as base of "plastic" zone (shaded). Distribution of normal stress along load axis shown according to Hill's elastic/plastic solution (broken curve) and present approximation (full curve).

pressure, as determined by the material hardness, so that

$$\sigma_m = \theta H \approx \text{const.}, \quad (2)$$

with θ a dimensionless factor: hardness is thus the key scaling parameter that establishes the intensity of the stress. The spatial extent of the field must scale with the indentation size, as determined by the characteristic contact dimension a (or d), giving

$$b = \eta a = (\eta^2/\alpha\pi H)^{1/2} P^{1/2}, \quad (3)$$

with η another dimensionless factor.

Now we consider the initiation of fracture within the stress field. For this purpose we investigate the mechanics of a median-plane penny crack of radius c centred on the load axis at the base of the elastic/plastic interface. In line with the linear distribution proposed above, the stresses over the prospective crack plane are taken to be symmetrical about the penny axis according to the radial function

$$\sigma(r) = \sigma_m(1 - r/b) \qquad (r \leqslant b) \quad (4a)$$

$$\sigma(r) = 0 \qquad (r \geqslant b). \quad (4b)$$

More complex stress fields that include the angular dependence of the stress about the elastic/plastic interface, the compressive stress in the plastic zone at $r > b$ etc., can be used, but such refinements yield essentially the same final result as that obtained using the much simpler field represented by Equation 4. The present description requires the pre-existence of nucleation centres within the bulk of the specimen, such that if one favourably located centre does not develop into a full-scale median crack the expanding plastic zone will engulf this nucleus and "search" for another. While a more deeply located flaw would not experience a greater maximum in tensile stress, Equation 2, it would certainly experience a greater overall tension averaged over its length, Equation 3. Our aim is to determine the loading conditions at which the "dominant flaw" becomes critical.

This is most readily done by evaluating the stress intensity factor for axially symmetric penny cracks [11],

$$K = [2/(\pi c)^{1/2}] \int_0^c r\sigma(r)\mathrm{d}r/(c^2 - r^2)^{1/2}. \quad (5)$$

Substitution of Equation 4 into this integral gives

$$K = 2\sigma_m(c/\pi)^{1/2}[1 - \tfrac{1}{2}(1 - b^2/c^2)^{1/2} - \tfrac{1}{2}(c/b)\sin^{-1}(b/c)], \quad (c \geqslant b), \quad (5a)$$

$$K = 2\sigma_m(c/\pi)^{1/2}(1 - \pi c/4b), \quad (c \leqslant b). \quad (5b)$$

Invoking the condition for Griffith equilibrium,

$$K = K_c, \quad (6)$$

and using Equations 2 and 3 to eliminate σ_m and b, Equations 5 lead to critical relations for crack extension: in reduced notation we obtain

$$1 = \mathscr{C}^{1/2}[1 - \tfrac{1}{2}(1 - \mathscr{P}/\mathscr{C}^2)^{1/2} - \tfrac{1}{2}(\mathscr{C}/\mathscr{P}^{1/2})\sin^{-1}(\mathscr{P}^{1/2}/\mathscr{C})], \quad (\mathscr{C} \geqslant \mathscr{P}^{1/2}), \quad (7a)$$

$$1 = \mathscr{C}^{1/2}(1 - \pi\mathscr{C}/4\mathscr{P}^{1/2}), \quad (\mathscr{C} \leqslant \mathscr{P}^{1/2}) \quad (7b)$$

where we have made the convenient substitutions

$$\mathscr{C} = (2\theta H/\pi^{1/2}K_c)^2 c \quad (8a)$$

$$\mathscr{P} = (16\eta^2\theta^4 H^3/\alpha\pi^3 K_c{}^4)P. \quad (8b)$$

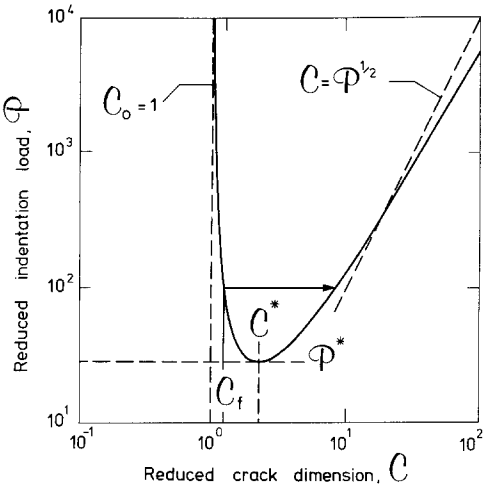

Figure 3 Plot of equilibrium function $\mathscr{P}(\mathscr{C})$, showing development of flaw into full-scale crack at threshold (arrow).

The formulation thus uniquely relates equilibrium crack dimensions to the indentation load.

Accordingly, in solving Equation 7 for the "universal" function $\mathscr{P}(\mathscr{C})$, we lay down the basis for tracing the evolution of the initiation process. The plot of Fig. 3 indicates the sequence of events for a dominant flaw of "effective" initial dimension $\mathscr{C}_f$. Upon loading the indenter, the flaw experiences an increasing driving force until, at the load where the line $\mathscr{C}_f = \text{const.}$ intersects the equilibrium curve, the Griffith condition for extension becomes satisfied. The flaw is then free to develop into a median crack. Noting that the $\mathscr{P}(\mathscr{C})$ curve has a minimum at $(\mathscr{P}^*, \mathscr{C}^*)$, where

$$\mathscr{C}^* = 2.250 \tag{9a}$$

$$\mathscr{P}^* = 28.11, \tag{9b}$$

and an asymptote to $\mathscr{C}_0 = \text{const.}$, where

$$\mathscr{C}_0 = 1, \tag{10}$$

we may identify three distinct regions of stability in the flaw size:

(i) $\mathscr{C}_f \leqslant \mathscr{C}_0$ (small flaws): It is impossible for the line $\mathscr{C}_f = \text{const.}$ to intersect the equilibrium curve, so the flaw can never expand. Physically, this situation arises because of the limitation on the stress level imposed by the hardness value, Equation 2, so that a small flaw, even with the maximum tensile stress distributed over its entire area (i.e. at $b \to \infty$, $P \to \infty$, Equation 3), simply cannot achieve the critical stress intensity factor.

(ii) $\mathscr{C}_0 < \mathscr{C}_f < \mathscr{C}^*$ (intermediate flaws): The line $\mathscr{C}_f = \text{const.}$ now intersects the equilibrium curve on the branch of negative slope, i.e. the unstable branch, such that development into the median crack is spontaneous at $P = \text{const.}$ It is this case which is represented in Fig. 3, and which corresponds to the empirically observed threshold condition. While the total stress fall-off over the radius of the crack at critical loading increases as the flaw size within this range, the system is never too far removed from the highly unstable uniform-tension configuration [12].

(iii) $\mathscr{C}^* \leqslant \mathscr{C}_f$ (large flaws): intersection occurs on the branch of positive slope, so further development can only take place by stable growth along the equilibrium curve at increasing load. The appearance of a median crack is then a continuous rather than abrupt event. Total stress fall-off over the crack is now severe, so that the critical system more closely resembles a highly stable centre-loading configuration [12].

It is clear from this description that crack initiation will depend to a large extent on the distribution in effective size and location of potential starting flaws. In the absence of large flaws, the indentation will expand until a suitable intermediate flaw is encountered and taken to threshold before being engulfed within the plastic zone. However, while this must inevitably lead to variability in the critical loading, it is clear from Fig. 3 that *no* flaw, regardless of its favourable size or location, may extend, either unstably or stably, at indentation loads below $\mathscr{P}^*$. Thus the minimum in the equilibrium curve takes on a special significance, in that it represents a lower bound to the requirements for initiation. At this point on the curve the indentation variables are obtained in absolute terms from Equations 8 and 9:

$$C^* = (1.767/\theta^2)(K_c/H)^2 \tag{11a}$$

$$P^* = (54.47\alpha/\eta^2\theta^4)(K_c/H)^3 K_c. \tag{11b}$$

3. Discussion

The model described above, while ostensibly dealing with crack initiation processes, makes no assumptions about the nature of starting flaws other than that they exist and have some "effective" dimension: in seeking to establish a well-defined crack system we have concentrated on the *formation*, as distinct from the *nucleation*, of indentation microcracks [12]. It is nevertheless apparent that appropriate refinement of micro-

TABLE I Parameters (approx.) of indentation fracture initiation

Material	Comments	Deformation/fracture parameters		Threshold parameters	
		H (GPa)	K_c(MPa m$^{1/2}$)	P^* (N)	c^* (μm)
WC	Co-bonded	18.6	13	96	22
NaCl	monocrystal	0.24	0.4	40	120
Si_3N_4	hot-pressed	16	5	3	4
Al_2O_3	lucalox	12	4	3	5
ZnS	vapour deposited	1.9	1.0	3	12
SiC	hot-pressed	19	4	0.8	2
MgF_2	hot-pressed	5.8	0.9	0.07	1.1
MgO	hot-pressed	9.2	1.2	0.06	0.8
SiO_2	glass	6.2	0.7	0.02	0.6
Si	monocrystal	10	0.6	0.003	0.2

structure (e.g. refinement of grain size in polycrystals, reduction of pile-up length in monocrystals, elimination of micro-inhomogeneities in glasses) could be an important factor in the design and manufacture of ultra-high strength ceramics for contact situations. In the context of indentation fracture, the micro-mechanics of nucleation processes remains a relatively unexplored area of study.

Of greater interest than flaw characteristics, however, is the role of the basic deformation/fracture parameters, hardness and toughness, in controlling the intrinsic resistance to the onset of contact-induced cracking. For the purpose of materials selection, one would aim to maximize the quantities P^* and c^*; i.e. one would look for materials of high toughness, low hardness, as per Equations 11. The importance of these two basic material parameters in determining the question of "brittleness" has been previously noted in other aspects of the indentation fracture problem [5, 7, 8]. Because of the simplifying assumptions embodied in the model of Fig. 2, absolute evaluations of P^* and c^* can hardly be expected to have an accuracy of much better than an order of magnitude; on the other hand, since all the inaccuracy in the theory is contained in the constants in Equations 11, relative values will be limited only by experimental uncertainties in H and K_c. Table I accordingly lists the appropriate quantities for a selection of solids, using $\alpha = 2/\pi$ (Vickers diamond pyramid indenter, with a measured as impression diagonal), $\theta \approx 0.2$ and $\eta \approx 1$ (typical intensity and extent of tensile field). Those solids toward the upper portion of the table would appear to be favoured candidates for applications in which the onset of cracking means an immediate, significant degradation in properties. Of course, once full-scale cracking has begun it is the toughness which becomes the optimizing parameter.

Acknowledgements

This work was funded by the Australian Research Grants Committee and the U.S. Office of Naval Research under contract No. N00014-75-C-0669.

References

1. B. R. LAWN and T. R. WILSHAW, *J. Mater. Sci.* **10** (1975) 1049.
2. A. G. EVANS and T. R. WILSHAW, *Acta. Met.* **24** (1976) 939.
3. *Idem, J. Mater. Sci.*, **12** (1977) 97.
4. F. C. FRANK and B. R. LAWN, *Proc. Roy. Soc. Lond.* **A299** (1967) 291.
5. B. R. LAWN and M. V. SWAIN, *J. Mater. Sci.* **10** (1975) 113.
6. B. R. LAWN and E. R. FULLER, *ibid.* **10** (1975) 2016.
7. B. R. LAWN, T. JENSEN and A. ARORA, *ibid.* **11** (1976) 575.
8. A. G. EVANS and E. A. CHARLES, *J. Amer. Ceram. Soc.* **59** (1976) 371.
9. R. HILL, "Plasticity" (Clarendon Press, Oxford, 1950) p. 97.
10. D. TABOR, "The Hardness of Metals" (Clarendon Press, Oxford, 1951).
11. G. C. SIH, "Handbook of Stress Intensity Factors" (Lehigh University Press, Lehigh, 1973).
12. B. R. LAWN and T. R. WILSHAW, "Fracture of Brittle Solids" (Cambridge University Press, Cambridge, 1975) Chs. 1–3.

Received 16 March and accepted 4 April 1977.